Tellus (1984), *36A*, 355–368

Stratocumulus instability reconsidered: a search for physical mechanisms

By HOWARD P. HANSON, *Cooperative Institute for Research in Environmental Sciences, University of Colorado, Boulder, CO 80309, USA*

(Manuscript received November 18, 1983; in final form February 8, 1984)

ABSTRACT

Conditions under which stratocumulus cloud decks become unstable and break apart into patchy trade cumulus are investigated using observations made over the Pacific and a theoretical analysis with a mixed-layer model. That the criterion that cloud-top entrainment fluxes be turbulence-generating is sufficient for instability is found to be overstated: it appears from the observations either that solid cloud decks can support positive entrainment buoyancy fluxes or that the criterion is simply impossible to measure due to inherent uncertainties about cloud-top structure. The former conclusion is also supported by the model analysis. Other criteria for stratocumulus instability are sought, and it is concluded that further numerical experiments are necessary to establish certainty about the process.

1. Introduction

The persistent stratus and stratocumulus (Sc) cloud decks that occur on the eastern sides of the subtropical anticyclones over the Atlantic and Pacific Oceans in both hemispheres have been the subject of considerable research in recent years. Much of this research has been stimulated by the clouds' rôles as radiatively active feedback mechanisms in the global climate system. Positioned approximately astride the Tropics of Cancer and Capricorn, they reflect sunlight that would otherwise contribute significantly to oceanic heating. The cold water—relative to the zonal average at the same latitudes—off the west coasts of North and South America and Africa is maintained at least in part by the presence of the cloud decks. Small ocean temperature increases have been shown to cause the Sc clouds to act as a negative feedback mechanism by reducing ocean heating (Hanson and Gruber, 1982), since the clouds become thicker and more reflective, *as long as the cloud deck remains solid.* The break-up of a solid Sc deck, however, may change the sign of this feedback by allowing further oceanic heating of warm anomalies. In particular, the size of the Sc decks must play an important rôle in the net heating of the subtropical oceans through this feedback mechanism. This paper concerns the processes by which the solid Sc decks break apart into partly-cloud-covered trade cumulus cloud fields at their downwind edges.

The size of these Sc decks appears to be governed by an instability process that leads to their breakup toward the equator along trajectories around the eastern side of the subtropical anticyclones. During its passage through the Sc regime along such a trajectory, an air column is subject to increasing surface heat and moisture fluxes, due to increasing sea surface temperatures, and to decreasing suppression by large-scale subsidence. Consequently, the Sc-topped boundary layer becomes deeper and warmer; eventually, the subsiding air above the trade-wind inversion becomes unstable (in some sense) with respect to the boundary layer air, and the solid deck breaks apart. In addition to controlling the size of the solid cloud decks and their rôle in climate, the nature of this instability process is important because there is some indication that the size of these Sc decks reflects changes in the large-scale trade-wind circulation (Kraus and Leslie, 1982).

Lilly (1968) suggested that this instability occurs simply as conditional instability; i.e., in the presence of an upward decrease of equivalent potential temperature at the cloud top, the cloud becomes unstable. Randall (1976, 1980) and Deardorff (1980) showed that including the effects of cloud water on buoyancy allows stability in the presence of small equivalent potential temperature decreases at cloud top, and they derived an instability criterion based on (various linear combinations of) the cloud-top changes of temperature and water substance. Randall's (1980) discussion of the process as a "conditional instability of the first kind upside down" showed it to be associated with cloud-top entrainment fluxes that produce turbulence kinetic energy (TKE) contrary to the usual case in which they produce potential energy at the expense of TKE. Deardorff's (1980) mixing diagrams illustrate the process clearly: during mixing of cloud-top and above-inversion air, the evaporative cooling of cloud droplets into the mixture can produce a parcel of greater density than the surrounding cloud-top air, and the parcel will therefore sink into the cloud before it becomes saturated. This is the basis of the instability criterion. Deardorff suggested that this will tend to break apart the solid cloud and referred to the process as "cloud-top entrainment instability". He also presented results from an integration of a fine-resolution, three-dimensional planetary boundary layer (PBL) model in which the instability was forced to occur (by artificially cooling the air above the inversion) that showed a tendency for the cloud to break apart from the base upward. Moeng and Arakawa (1980) used a coarse-resolution two-dimensional model to investigate the development of the Sc-topped PBL in the aforementioned trajectories; in their results, the solid cloud was seen to break up toward the southwest in rough correspondence to onset of the instability criterion developed by Randall. Their horizontal resolution (10 km) was far too coarse, however, to yield insight into the actual process, which seems to occur on the scale of the cloud thickness. (This distinguishes, therefore, between unstable Sc decks and mesoscale cellular convection.) Moeng (1979) reported a linear stability analysis of a cloud-topped mixer-layer model in which basic states fulfilling Lilly's instability criterion were shown to be unstable to small perturbations. This is consistent with the corrected criterion, since she neglected liquid water effects on buoyancy in the linear analysis. She also showed the mechanics of the linear instability to correspond to the discussions of Randall and Deardorff.

There is little doubt that when this "instability" occurs, the energetics of the PBL change, but it is not clear that the onset of the instability suffices to break apart a solid Sc deck. This was asserted by Hanson (1982a) who argued that the sinking of parcels into the cloud *top* and their generation of TKE does not necessarily imply that the parcels must sink entirely *through* the cloud. Evidence, unfortunately, is scant, because of inherent difficulties in measuring cloud entrainment directly and other complications. Mahrt and Paumier (1982), for example, discussed measurements of cloud-top instability taken during the air-mass transformation experiment above broken Sc. They made four calculations of the cloud field's stability—based on Deardorff's (1980) analysis—from various portions of their turbulence record and an aircraft sounding: All four indicated instability, but the variability was large. On this basis, they doubted the usefulness of simple "jump" inversion criteria. Hanson (1984) discussed aircraft measurements of the solid Sc deck off California in which the layer was quite well-mixed. Despite the fact that the cloud was non-broken, both soundings and horizontal averaging runs discussed further in Subsection 2.2 below indicate a marginally stable cloud, with variability similar to that deduced by Mahrt and Paumier (1982) for "broken stratocumulus". Other soundings through the California Sc deck presented in Subsection 2.3 also show an inconclusive correspondence between Deardorff's and Randall's instability criterion and the brokenness of the cloud deck.

Operational use, whether for theoretical modeling or forecasting purposes, requires an instability criterion that is directly linked to the breakup of a solid cloud deck and provides sufficiency for the break-up process. Therefore, this paper makes an attempt to distinguish between the breakup process(es) (which will be referred to as *stratocumulus instability*) and the TKE generating processes discussed by Randall (1980) and Deardorff (1980). In Section 3 of this paper, the criterion developed by Randall and by Deardorff is reviewed and several other aspects of the cloud stratification and its relationship to the cloud-top instability are discussed; this is accomplished in the

context of a mixed-layer structure. Then, the mixed-layer entrainment closure of Stage and Businer (1981a,b) is used with the thermodynamic budget equations to investigate the processes that can lead to an actual instability of an Sc deck. Deardorff's (1980) numerical experiment is discussed at length. Section 4 contains a summary and a discussion of the need for carefully controlled experiments with a fine-resolution PBL model.

2. Data analysis

2.1. *Theoretical background*

The thermodynamic variables used here are based on water substance and moist static energy (an analog of equivalent potential temperature) in geometric height coordinates. Thus

$$r \equiv q + l, \tag{2.1}$$

where q and l are the mixing ratios of vapor and liquid water, respectively, and $l = 0$ if $q < q^*$, where q^* refers to the saturation value, and

$$h = Lq + c_p T + gz, \tag{2.2}$$

where T and z are temperature and height and the other symbols are defined in Appendix A. The two variables h and r completely describe the thermodynamic properties of an air parcel; they are also conserved during water phase changes.

Following Randall (1980), it is convenient to define a number of thermodynamic coefficients, all of which will be taken as constants in the theoretical analysis in Section 3, but will be allowed to vary in Section 2b:

$$\delta \equiv \left(\frac{\text{molecular weight of dry air}}{\text{molecular weight of water vapor}} - 1 \right) \simeq 0.61,$$

$$\varepsilon \equiv \frac{c_p T}{L} \simeq 0.12, \tag{2.3}$$

$$\gamma \equiv \frac{L}{c_p} \left(\frac{\partial q^*}{\partial T} \right)_p \simeq 1.6,$$

$$\beta \equiv \frac{1 + (1 + \delta)\varepsilon\gamma}{1 + \gamma} \simeq 0.5.$$

Various relationships among these coefficients and physical quantities relevant to the analysis below will arise: for example, it can easily be shown that the moist adiabatic lapse rate is $-\partial T/\partial z = \beta g/c_p$ and the corresponding gradient of virtual static energy (an analog of virtual potential temperature θ_v) is

$$\partial s_v/\partial z = g|1 - (1 + \delta)\varepsilon|(1 - \beta) \equiv g'. \tag{2.4}$$

The criterion for instability of an Sc deck developed by Randall and Deardorff is written here using Stage and Businger's (1981a, b) notation as

$$\Delta_2 = \beta(h_U - h_B) - \varepsilon L(r_U - r_B) < 0. \tag{2.5}$$

Here $(\ )_U$ and $(\ )_B$ values are just above the cloud-top in clear air and just within the uppermost part of the cloud, respectively. (The quantity Δ_2/c_p is the analog of the stability index used by Mahrt and Paumier, 1982.) This paper follows Deardorff's (1980) terminology and refers to cases of $\Delta_2 < 0$ as cloud-top entrainment instability (CEI). Randall (1980) showed that

$$\Delta_2 = \Delta s_v - \Delta s_v^*, \tag{2.6}$$

where $\Delta s_v = s_{v_U} - s_{v_B}$ is the cloud-top virtual static energy jump and

$$\Delta s_v^* = \frac{1 - \beta}{\gamma} L(q_U^* - q_U). \tag{2.7}$$

Randall calls this the "critical value" of Δs_v, which increases with decreasing relative humidity of the above-inversion air. If $\Delta s_v < \Delta s_v^*$, CEI occurs.

Another relevant s_v difference that will be important is

$$\Delta_1 \equiv (h_U - h_M) - (1 - \varepsilon\delta)L(r_U - r_M). \tag{2.8}$$

which is applicable to discontinuous inversions between two *clear* layers; the notation $(\ )_M$ will generally refer to mixed-layer values, but Δ_1 refers to a physical s_v difference only if h_M and r_M are unsaturated. In an Sc-topped mixed layer with cloud base z_C and cloud top z_B,

$$\Delta s_v = s_{v_U} - s_{v_B} = \Delta_2 + \Delta s_v^* = \Delta_1 + g'(z_B - z_C), \tag{2.9}$$

whence

$$\Delta_1 - \Delta_2 = g'(z_B - z_C) + \Delta s^* \tag{2.10}$$

Physically, $g'(z_B - z_C)$ is the s_v *increase* upward through the cloud deck and can be shown via the identities used above to be related to the cloud-top liquid water mixing ratio:

$$g'(z_B - z_C) = |1 - (1 + \delta)\varepsilon|Ll_B. \tag{2.11}$$

Thus the s_v increase through the cloud is related to cloud-top *over-saturation*, because $l_B = r_B - q_B^*$. Since Δs^* is the s_v *deficit* of the above-inversion air relative to its saturation s_v, it is proportional to the upper-air *under-saturation*. More generally, the definition of Δ_1 stems from the definition of s_v in under-saturated air:

$$s_v = h - (1 - \varepsilon\delta)Lr = gz + c_pT + \delta\varepsilon Lr \simeq c_pq_v. \tag{2.12}$$

2.2. *Day 178/1981*

The data set analyzed here was obtained in late June and early July, 1981 using a NOAA P-3. Day 178 (June 27) is the day discussed in Hanson (1984); that paper also contains a description of instrumentation. It was shown that saturation point mixing lines on a tephigram implied marginally stable mixing; here a numerical analysis is performed using a variety of assumptions.

Two sets of averaging runs were conducted near the cloud top; each set consisted of a run within the cloud and a run just above the inversion, which was well defined and ~50 m thick. Each of the four runs lasted ~5 min, covering ~30 km. Other sets for which the two runs were at identical altitudes showed that this procedure sampled effectively the same air mass during each set; in the two sets discussed here (#'s 5 and 8 in Hanson, 1984), one run measured $(\ )_B$ quantities and the other $(\ )_U$ quantities. Table 1 shows these averaged measurements. The last two lines in Table 1 contain water vapor and liquid water values corrected for the fact that runs 5a and 8b were within the inversion; this is clear from the profiles in Fig. 3 of Hanson (1984).

Table 1. *Averaged measurements, day 178/1981*

Run	Level	$\bar{z}(m)$	$\bar{p}(hPa)$	$\bar{T}(K)$	$\bar{q}$(g kg^{-1})	l(g kg^{-1})
5a	B	934.0	907.1	286.1	6.4	0.18
5b	U	979.7	902.3	293.3	2.8	0.0
8a	U	983.0	901.4	294.2	2.1	0.0
8b	B	921.2	907.1	285.5	6.8	0.18
5a′	B	934.0	907.1	286.1	8.0	0.72
8b′	B	921.2	907.1	285.5	8.0	0.92

The cloud-top stability in terms of CEI on day 178 is assessed in Table 2 using several calculations of Δ_2. Estimates 1A (ascent) and 1D (descent) are made from runs 5 and 8 in Table 1, respectively. The values of Δ_2/c_p indicate stability; however, when the variability of the measurements is taken into account (fifth column), it is seen that portions of the record must have been unstable. Estimates 2A and 2D use averages from the sub-cloud layer averaging runs for the $(\ )_B$ values, implying a mixed-layer assumption. In this case, the variability is much lower, although the descent case may contain some instability. Estimates 3A and 3D use the corrected moisture values from Table 1, and the cloud is subject to instability. From these averaged measurements, assessment of cloud-top stability is ambiguous. Estimates 4 and 5 in Table 2 utilize thermodynamic values taken from the vertical profiles presented in Hanson (1984);

Table 2. *Cloud-top stability, day 178/1981*

Estimate	Δh (kJ kg^{-1})	Δr (g kg^{-1})	Δ_2/c_p (K)	σ(K)
1A	−1.21	−3.78	0.50	3.20
1D	−2.26	−4.88	0.28	2.08
2A	−1.87	−5.93	0.80	0.48
2D	−3.96	−6.83	0.10	0.49
3A	−5.16	−5.92	−0.81	—
3D	−5.22	−6.82	−0.62	—
4A	−3.97	−6.46	−0.23	—
4D	−4.07	−6.66	−0.19	—
5A	−3.21	−6.20	0.32	—
5D	−4.09	−6.70	0.08	—

estimates 4 use inversion base values and 5 use mixed-layer values. These results are quite similar to estimates 3 and 2, respectively; it can be inferred that the relevant variability for the mixed-layer cases (as measured by σ) is at least of the order 0.5 K. The point of this exercise is two fold: first, it demonstrates the difficulty of obtaining precise values of Δ_2 (a point stressed by Mahrt and Paumier, 1982), and, second, it shows that using a mixed-layer assumption from profile measurements (i.e., estimates 5) provides a reasonable and somewhat conservative estimate of Δ_2, compared to the other assumptions.

2.3. *Aircraft soundings*

In addition to the "race track" flight of June 27, "trajectory" flights were made on June 26, 28 and July 4, 9, 1981 (Julian Days 177, 179, 185, 190, respectively). These flights consisted of a stair-step pattern of averaging runs at various levels with

smooth descents between sets. Further details are available in Hanson (1982b). These descents provide sounding information in a variety of Sc cloud situations. In addition the character of the Sc clouds—solid, broken, patchy—has been determined from a combination of the on-board 16 mm films and observer logs. 21 soundings (including the 2 on June 27) are thus available for analysis; of these, 6 are clearly in the category of "broken" Sc and two classify as "patchy". In Table 3, these soundings are labelled with a 4-digit number, with the first 3 digits being the Julian Day and the last the sounding number. In the second column, S means "solid" and B and P mean "broken" and "patchy", respectively. (The difference between the latter two categories is based on the scale of the clear areas. "Patchy" implies large, relatively flat cloud masses well-separated while "broken" refers to a relatively homogeneous—on the observer scale of several kilometers—cloud with holes through which the ocean was visible.) The two patchy cases in Table 3 consisted of what appeared to be mesoscale cellular convection, and the descent profile was made through a cloudy area.

Table 3. *Cloud-top stability, EPOCS-1981 profiles*

Profile	Cloud	Δh (kJ kg^{-1})	Δr (g kg^{-1})	Δ_2/c_p (K)
1774	B	−9.88	−8.14	−2.61
1775	B	−2.14	−4.81	0.30
1776	B	−0.61	−3.86	0.77
1781	S	−3.21	−6.20	0.32
1782	S	−4.09	−6.70	0.08
1791	S	1.65	−4.19	2.06
1792	S	3.84	−3.54	3.04
1793	S	−1.61	−5.80	0.76
1794	S	−4.96	−6.75	−0.76
1795	B	−7.31	−6.21	−2.25
1851	S	−0.64	−5.72	1.22
1852	S	−1.62	−4.93	0.41
1853	S/P	−3.51	−5.80	−0.40
1854	B	−5.16	−6.13	−1.17
1856	B	−0.61	−5.15	1.07
1901	S	−5.74	−6.66	−1.11
1902	S/P	−3.84	−5.97	−0.37
1903	S	0.25	−4.35	1.36
1904	S	1.92	−2.56	1.71
1906	S	−6.58	−7.25	−1.51
1907	S	−6.07	−7.11	−1.20

The last column of Table 3 gives values of Δ_2/c_p from mixed-layer measurements for the in-cloud values as in estimates 5 of Table 2. Table 4 is a contingency chart showing averages and standard deviations from Table 3 for the four possible categories. Although there is agreement with the general precept that larger, *positive* values of Δ_2 occurred in solid clouds and larger *negative* values in broken clouds, the "anomalous" cases (i.e. $\Delta_2 > 0$, broken and $\Delta_2 < 0$, solid) make it difficult to believe that $\Delta_2 < 0$ is a sufficient criterion for Sc break-up. The last line of Table 4 reassigns the two S/P cases (profiles 1853 and 1902) to "B": this only increases the uncertainty. Whether this insufficiency is because of physics or observational uncertainty is unclear. The next step is to investigate the physics, since the uncertainty is endemic.

Table 4. *Averages from Table 3, by category, showing # of cases [average Δ_2/c_p (K); s.d. (K)]*

	S	B
$\Delta_2/c_p > 0$	9 (1.22; 0.95)	3 (0.71; 0.39)
$\Delta_2/c_p < 0$	6 (−0.89; 0.50)	3 (−2.01; 0.75)
(see text)	3 (−1.16; 0.38)	5 (−1.36; 1.04)

3. Theoretical analysis

3.1. *Mixing of two parcels*

Since h and r are conservative for water phase changes, constant height mixing produces parcels with (h, r) values intermediate to those of the two parcels being mixed (Hanson, 1981). Mixing between above-inversion air and mixed-layer air thus produces intermediate parcels

$$(h_1, r_1) = f_U(h_U, r_U) + f_M(h_M, r_M), \tag{3.1}$$

where f_U and f_M are the fractional amounts of upper and mixed layer air in the intermediate parcel; it is assumed that $f_U + f_M = 1$, so that

$$(h_1, r_1) = (h_M, r_M) + f_U(\Delta h, \Delta r). \tag{3.2}$$

Now, mixing diagrams constructed by Deardorff (1980) and Hanson (1981, 1982a) show that during this cloud-clear air mixing, the parcels with lowest s_v (i.e., highest density) occur just at saturation. Therefore, attention is restricted to these just-saturated cases: $h_1 = h_1^*$; $r_1 = q_1^*$ and f_U is the fraction of upper air in such a just-saturated

mixture. Since $(\ )_I$ is just saturated, its s_v difference with the sub-cloud air is

$$s_{v_I} - s_{v_M} = (h_I - h_M) - (1 - \varepsilon\delta)L(r_I - r_M) = f_U\Delta_1. \quad (3.3)$$

Clearly, if $s_{v_I} - s_{v_M} < 0$, the cloud will indeed be unstable as the intermediate parcels will be capable of sinking all the way to the surface. Within the cloud,

$$s_v(z) = s_{v_M} + g'(z - z_C), \quad (3.4)$$

so that

$$s_{v_I} - s_v(z) = f_U\Delta_1 - g'(z_B - z_C)\hat{z}, \quad (3.5)$$

where $\hat{z} \equiv (z - z_C)/(z_B - z_C)$ is a non-dimensional height within the cloud.

In so far as $(\ )_I$ is just saturated, its s_v difference with the cloud-top air can be written (following Randall, 1980):

$$s_{v_I} - s_{v_B} = \beta(h_I - h_B) - \varepsilon L(r_I - r_B) = f_U\Delta_2, \quad (3.6)$$

where the last equality follows from the mixed-layer assumption that $h_B = h_M$; $r_B = r_M$. Suppose a neutral level within the cloud (or above it, along its extrapolated s_v structure) is defined such that

$$s_{v_I} - s_v(\hat{z} = \psi) \equiv 0. \quad (3.7)$$

Then

$$f_U\Delta_1 = g'(z_B - z_C)\psi, \quad (3.8)$$

and

$$f_U\Delta_2 = f_U\Delta_1 - g'(z_B - z_C) = -g'(z_B - z_C)(1 - \psi). \quad (3.9)$$

Furthermore,

$$f_U(\Delta_1 - \Delta_2) = g'(z_B - z_C), \quad (3.10)$$

which, with eq (2.10), gives

$$f_U = \frac{g'(z_B - z_C)}{g'(z_B - z_C) + \Delta s_v^*}. \quad (3.11)$$

This can be re-written as

$$f_U = [1 + (q_U^* - q_U)/(1 + \gamma)/l_B]^{-1}, \quad (3.12)$$

Hence, larger values of Δs_v^* (drier upper air) are associated with lower values of f_U, since the $(\ )_I$ parcel requires more water (cloud air) to become saturated. Thus,

$$\Delta_1 = [g'(z_B - z_C) + \Delta s_v^*]\psi, \quad (3.13)$$

$$\Delta_2 = -[g'(z_B - z_C) + \Delta s_v^*](1 - \psi).$$

A neutral level *within* the cloud, $0 < \psi < 1$ therefore implies

$$\Delta_2 < 0 < \Delta_1,$$

and such a level "above" the cloud implies

$$0 < \Delta_2 < \Delta_1.$$

The CEI discussed by Randall (1980) and by Deardorff (1980) occurs when $\psi < 1$. As suggested above, $\psi > 0$ is required for static stability of the upper air with respect to the sub-cloud layer. It also seems quite likely that $\Delta s_v > 0$ is required for cloud stability (so that the upper air and upper part of the cloud do not overturn); this restricts Δ_1 and Δ_2 such that

$$\Delta_1 > g'(z_B - z_C), \quad (3.14)$$

$$\Delta_2 > -\Delta s_v^*,$$

and also produces the compact result that, for stability,

$$\psi > f_U. \quad (3.15)$$

Table 5. *"Unstable" profile data*

Profile	$g'(z_B - z_C)$ (kJ kg^{-1})	s_v^* (kJ kg^{-1})	f_U	ψ
1774*	0.53	12.22	0.04	0.69
1794	1.72	10.85	0.14	0.85
1795*	1.24	8.45	0.13	0.72
1853**	0.79	10.68	0.07	0.86
1854*	0.52	10.74	0.05	0.79
1901	0.52	11.59	0.04	0.79
1902**	0.54	11.16	0.05	0.84
1906	1.07	11.95	0.08	0.78
1907	0.98	11.98	0.08	0.79

* Indicates broken stratocumulus.
** Indicates patchy stratocumulus.

Table 5 shows values of $g'(z_B - z_C)$, Δs_v^*, ψ and f_U for the $\Delta_2 < 0$ aircraft soundings of Table 3. It can be seen, by comparison with Table 3, that the broken cases are stable in the sense that $\Delta s_v > 0$ (i.e., $f_U < \psi$). This occurs because $\Delta s_v^* \gg g'(z_B - z_C)$; i.e., the under-saturation of the upper air is far larger than the over-saturation (in the form of liquid water) of the cloud-top air (see eqs. 2.7 and 2.11).

3.2. *Mixed-layer model analysis*

3.2.1. *Model.* This analysis investigates two

specific processes that could lead to stratocumulus instability in the simplest possible model; the first of these is the possibility of runaway entrainment, i.e., $w_e \to \infty$. Of course, the Sc-topped mixed-layer model cannot adequately describe partly cloudy situations, so stratocumulus instability in the model implies a condition in violation of a model assumption. This will be discussed in (3.2.4) below.

The form of the mixed layer model used here stipulates surface turbulent fluxes, the cloud-top radiative flux and all advections. The surface-flux dependence on mixed-layer quantities is a negative feedback (damping) mechanism (i.e., for example, an upward moisture flux moistens the layer which in turn would tend to decrease the flux) so no instabilities will be submerged by this procedure. Accordingly,

$$\frac{d}{dt} h_M \equiv \dot{h}_M = (w_e \Delta h + F_h - F_R)/z_B,$$

$$\frac{d}{dt} r_M \equiv \dot{r}_M = (w_e \Delta r + F_q)/z_B, \tag{3.16}$$

where F_R is the cloud-top radiative flux, F_h, F_q are the surface moist static energy and water vapor fluxes and w_e is the entrainment rate. The simplest form of radiative flux distribution will be used—a jump from zero to F_R just below cloud top—without loss of qualitative generality. The surface fluxes will be stipulated via the moisture flux and a Bowen ratio, so that $F_h = LF_q(1 + B_0)$. The budgets above will be treated in Lagrangian form to avoid the complication of horizontal advections; the alternative interpretation is, of course, the assumption of horizontal homogeneity.

The entrainment closure of Stage and Businger (1981a, b) hypothesizes that the generation of TKE by positive buoyancy fluxes is balanced by the sum of potential energy generation and dissipation. For the Sc-topped mixture layer, this balance can be written as

$$w_e = \mathbf{F}/\Psi, \tag{3.17}$$

where the forcing $\mathbf{F}$ has contributions from the surface fluxes and the cloud-top cooling:

$$\mathbf{F} = \xi(2 - \xi)A_1F_1 + (1 - \xi)^2A_2F_2 + |\xi^2 + \beta(1 - \xi^2)|A_RF_R, \tag{3.18}$$

where

$$\xi \equiv z_c/z_B,$$

$$F_1 \equiv F_h - (1 - \varepsilon\delta)LF_q = LF_q(B_0 - \varepsilon\delta), \tag{3.19}$$

$$F_2 \equiv \beta F_h - \varepsilon LF_q = LF_q(\beta B_0 + \beta - \varepsilon),$$

and

$$A_{1,2,R} \equiv \begin{cases} A & F_{1,2,R} > 0, \\ 1.0 & F_{1,2,R} \leqslant 0, \end{cases} \tag{3.20}$$

with $(1 - A) \simeq 0.8$ the dissipation.

The denominator of eq. (3.17) represents essentially an overall layer stability,

$$\Psi \equiv \xi^2\Delta_1 + A'(1 - \xi^2)\Delta_2, \tag{3.21}$$

with

$$A' \equiv \begin{cases} A & \Delta_2 \leqslant 0, \\ 1.0 & \Delta_2 > 0. \end{cases} \tag{3.22}$$

Thus, CEL, occurring when $\Delta_2 < 0$, contributes to the entrainment rate by decreasing Ψ. The unbounded increase of w_e (i.e., runaway entrainment) occurs as $\Psi \to 0$. In terms of the inversion jumps, this occurs for

$$\Delta h \to L\Delta r/\alpha, \tag{3.23}$$

where

$$\alpha = \frac{|\xi^2 + A'(1 - \xi^2)\beta|}{\xi^2(1 - \varepsilon\delta) + A'(1 - \xi^2)\varepsilon}; \tag{3.24}$$

for $\xi = 0.5$, $\alpha = 0.9$. In contrast, $\Delta_2 \to 0$ as

$$\Delta h \to \varepsilon/\beta L\Delta r. \tag{3.25}$$

From eq. (3.24) it can be seen that $\Delta_2 = 0$ implies runaway entrainment only for a fog layer, $\xi = 0$. When the cloud base is elevated, TKE conversion to potential energy in the sub-cloud layer allows substantial negative values of Δ_2, in Stage and Bussinger's (1981a, b) closure (See Deardorff, 1980, Section 5 for further discussion of this point.)

3.2.2 *Stability analysis.* Stability tendencies can be examined using the behavior of Ψ. The analysis in Appendix B shows the derivation of a differential equation for Ψ for specified surface fluxes, radiation and cloud geometry:

$$\dot{\Psi} = \mathbf{F}(\Gamma_\theta - \Psi)/(\Psi z_B) - \mathbf{F}_\theta/z_B. \tag{3.26}$$

The steady-state value,

$$\Psi_0 = \Gamma_\theta/(1 + \mathbf{F}_\theta/\mathbf{F}), \tag{3.27}$$

allows this to be re-written as

$$\dot{\Psi} = -\frac{\Gamma_\phi \mathbf{F}}{z_B} \Psi_0 \left(\frac{\Psi - \Psi_0}{\Psi} \right). \tag{3.28}$$

This can be integrated analytically to give t as a transcendental function of Ψ; it is sufficient for the present purpose, however, simply to examine the differential equation above. Since Γ_ϕ and $\mathbf{F}$ are both positive, it becomes apparent that, for $\Psi_0^+ > 0$, Ψ_0^+ is a stable attractor for all positive initial Ψ, and, conversely, for $\Psi_0^- < 0$, $\Psi \to \infty$ with time. This is illustrated in Fig. 1. Hence there is no possibility

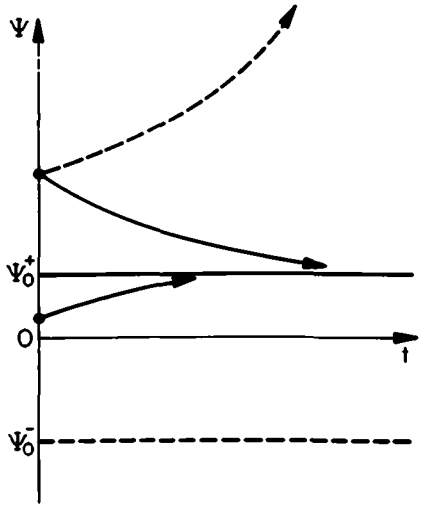

Fig. 1. Schematic behavior of eq. 3.28 for positive (solid) and negative (dashed) steady state values Ψ_0. Ψ_0^+ is an attractor and Ψ_0^- is a repellor of $\Psi(t)$.

of runaway entrainment, in the sense that $\Psi \to 0$, although a very small, positive Ψ_0 could lead to large entrainment. In particular, from the limits on Δ_1 and Δ_2 found previously in eqs. (3.14), if

$$0 < \psi_0 < g'(z_B - Z_c)\xi^2 - s_v^*(1 - \xi^2)A', \tag{3.29}$$

the attraction of Ψ_0 will cause the system to pass through a statically unstable state and this, while not constituting runaway entrainment *per se*, may be considered a stratocumulus instability. However, for all of the broken cases of Table 5, Δs_v^* is large enough to make the right-hand side of eq. (3.29) negative. This mechanism seems not to be at work in the 1981 data.

Nor does it appear to be involved in Deardorff's (1980) results. This numerical experiment forced CEI and subsequent stratocumulus instability by an artificial cooling of the above-inversion air (the physical analog of which is a sudden cold-air advection above the inversion). Within the framework of the present mixed-layer model, this is represented by the H_h term in eq. (B.1), and it enters the criterion above by reducing drastically the value of $\mathbf{F}_\phi$ and hence Ψ_0. Unlike the 1981 profile data, which is incomplete insofar as simultaneous values of the surface fluxes, radiative cooling, upper air vertical gradients and advections are unavailable, Deardorff's (1980) results allow calculation of values of Δs_v^* and Ψ_0 before and after the upper-air cooling and beginning of Sc break-up. Using Deardorff's profiles 1 and 6 for "before" and "after", respectively, numerical values from his Figs. 3, 4, 7 and 8 for fluxes and inversion values (there was no radiative flux in his experiment), and an average upper-air cooling of −3.3 K h^{-1} gives $\Psi_{0\text{before}} \sim 0.55$ kJ kg^{-1} and $\Psi_{0\text{after}} \sim -0.74$ kJ kg^{-1}. This change of sign indicates the overwhelming strength of the imposed cooling. At the same time, Δ_2 decreased from ~2.20 to ~−0.24 kJ kg^{-1}, indicating CEI, but Δs_v^* decreased from ~2.47 only to ~1.16 kJ kg^{-1}. Hence Deardorff's result is stable in the sense of eq. (3.29).

3.2.3. *Time-scale comparison.* Deardorff (1980) suggested a comparison of cloud moistening/drying time scales as a comprehensive criterion for instability. This can be examined analytically with the mixed-layer model. Given a free-convective velocity scale,

$$w_*^3 = C_1 \frac{g}{c_p \vartheta_R} \int_0^{z_B} \overline{w' s_v'} \, dz, \tag{3.30}$$

with $C_1 \simeq 2.5$, the time-scale for mixing within the cloud is $\tau_m = (z_B - z_C)/w_*$. The tendency for drying out due to entrainment of dry air above the inversion can be measured by the time scale $\tau_d = (z_B - z_C) l_B / (-w_e \Delta r)$, and the ratio of these is

$$\mathbf{T} \equiv \frac{\tau_m}{\tau_d} = \frac{w_e}{w_*} \left(1 + \frac{q_B - q_U}{l_B} \right). \tag{3.31}$$

Now, the entrainment closure used here is based on the vertically-integrated buoyancy fluxes, and the integral in eq. (3.30) is particularly simple. Limiting consideration to cases with $F_{1,2,R} > 0$,

$$\frac{2}{z_B} \int_0^{z_B} \overline{w' s_v'} \, dz = \mathbf{F}/A - w_e \, | \xi^2 \Delta_1 + (1 - \xi^2) \Delta_2 |. \tag{3.32}$$

Using eqs. (3.17) and (3.21), this is

$$\frac{2}{z_B}\int_0^{z_B}\overline{w's'_v}\,dz = \frac{1-A}{A}\cdot\frac{F}{\Psi} \times\left[\xi^2\Delta_1 + \frac{A'-A}{1-a}(1-\xi^2)\Delta_2\right]; \qquad (3.33)$$

the time-scale ratio is then

$$T = \left(1+\frac{q_B-q_U}{l_B}\right)\left(\frac{C_1 g z_B}{2c_p\vartheta_R}\,\frac{1-A}{A}\right)^{-1/3} w_e^{2/3}\left[\xi^2\Delta_1 + \frac{A'-A}{1-A}(1-\xi^2)\Delta_2\right]^{-1/3}. \qquad (3.34)$$

Using eqs. (3.13) and defining

$$C_2 = F^{2/3}\left[\frac{2Ac_p\vartheta_R}{(1-A)C_1 g z_B}\right]^{1/3}|g'(z_B - z_C) + \Delta s_v^*|^{-1}\left(1+\frac{q_B-q_U}{l_B}\right) \qquad (3.35)$$

gives

$$T = C_2|\xi^2\psi - A'(1-\xi^2)(1-\psi)|^{-2/3}\left[\xi^2\psi - \frac{A'-A}{1-A}(1-\xi^2)(1-\psi)\right]^{-1/3}, \qquad (3.36)$$

where

$$A' = \begin{cases} A & \psi \leqslant 1 \\ 1 & \psi > 1 \end{cases}. \qquad (3.37)$$

Fig. 2 shows T/C_2 as a function of ψ for $\xi = 0.5$. In Deardorff's (1980) numerical experiments, C_2 varied from $\sim 1.2\cdot 10^{-2}$ to $\sim 6\cdot 10^{-3}$ (profiles 1 and 6, respectively). The function T/C_2 shown in Fig. 2 varied correspondingly from ~ 0.4 to ~ 5.0 so T increased from $\sim 4.8\cdot 10^{-3}$ to $\sim 3\cdot 10^{-2}$. In contrast, using the flux data in Hanson (1984) and the profile data in Subsection 2B above (with an additional term in F to account for solar heating) gives an approximate value of $T \simeq 3.5\cdot 10^{-3}$ for the Day 178 data. The fact that $T < 1$ for Deardorff's profile 6 (an unstable one) is less important than its nearly order of magnitude increase over these two stable cases.

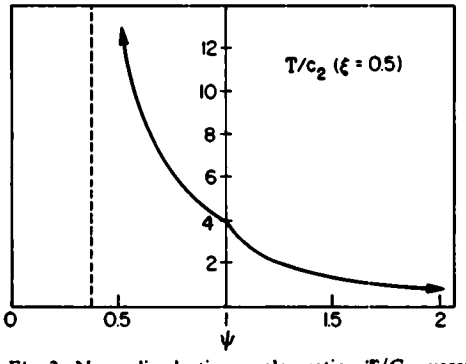

Fig. 2. Normalized time-scale ratio T/C_2 versus ψ showing increased drying for $\psi < 1 (\Delta_2 < 0)$.

The physical basis of this time-scale comparison can be understood from the perspective of the steady-state internal circulation of the well-mixed Sc-topped boundary layer. As first discussed by Schubert *et al.* (1979) and recently examined in some detail by Betts (1983), this circulation, in its simplest form, consists of approximately equal-area up- and down-drafts with the updrafts' transport of heat and moisture from the sea surface balancing the downdrafts' relatively dry and cool (due to the cloud-top radiation) transport. Since the water content varies more strongly than the temperature, the upward circulation branch is associated with a lower cloud base and the downward branch with a higher cloud base than the mean z_C (see Betts, 1983 Fig. 1). This bi-modal cloud base has a basis in the 1981 observations discussed in Section 2: "scud" was observed below the main stratocumulus deck in many of the cases of a deep layer ($\gtrsim 1$ km) which was nonetheless fairly well-mixed. Defining the descending-branch cloud base as z_{C_D}, it is straightforward to show that $(z_{C_D} - z_C)$ is directly proportional to T. Clearly, if $z_{C_D} > z_B$, the cloud cannot exist as a solid entity and stratocumulus instability occurs. It thus appears that the comparison of time scales may provide a useful diagnostic tool for stratocumulus instability, and the potential for a predictive criterion also exists on this basis.

3.2.4. *Decoupling.* One of the most significant aspects of Deardorff's (1980) numerical experiment was the decoupling of the cloud and subcloud turbulence after the onset of CEI. This is seen clearly in the water flux profiles (his Fig. 8) and, as pointed out in that paper, the non-linearity of these profiles implies that the layer can no longer be modelled as well-mixed. The analyses of the previous two subsections have conveniently neglected this fact; those analyses were intended to be

qualitative in nature, and the main conclusions are not likely to be changed. In particular, the non-linear fluxes increase F significantly for profile 6, further increasing T in that case. The nature of this decoupling is basic to the problem of stratocumulus instability, and the following discussion raises issues which can be addressed quantitatively only by detailed modeling.

The addition of TKE-generating processes at the top of a neutrally-stratified mixed layer is analogous to an increase of wind-stirring at the top of the oceanic mixed layer and results in enhanced turbulence levels throughout the layer and greater entrainment. In the case of the Sc-topped mixed layer, however, the increased TKE generation at the top can be impeded by the stratification lower down where $\partial s_v/\partial z > 0$. In this case, a second, quasi-mixed layer could tend to form in the upper part of the cloud just below the inversion and "entrain" its way downward in the (less turbulent) cloud below. Stratocumulus instability would then result from this new layer's deepening completely through the old cloud layer. This heuristic description is supported by the water flux profiles in Deardorff (1980): during the later stages of the integration, two quasi-linear flux regimes can be seen, one below and within the lower part of the cloud, where $\partial/\partial z(\overline{w'r'})$ is relatively unchanged throughout the integration, and one in the upper part of the cloud, where it is relatively constant with height and much larger than below. The question raised here is: does the onset of cloud-top entrainment instability and the growth of this new mixed layer necessary lead to stratocumulus instability? (In Deardorff's experiment, it did, of course.)

Two types of mixing from above may be distinguished: if $\Delta_2 < 0$ due to cooling of the above-inversion air, as in Deardorff's experiment, then the mixture will be saturated very near the cloud top and proceed to mix down into the cloud along the same stratification (gradient) as before but at lower values of s_v. In this case, there is nothing to stop the new mixed layer from eroding all the way through the cloud. The other possibility arises when $\Delta_2 < 0$ because of increasingly *dry* upper air. Then, the mixing proceeds downward at *constant* s_v, and, if it reaches its neutral buoyancy level before saturation the stratification becomes a factor. These two cases are schematically illustrated in Fig. 3.

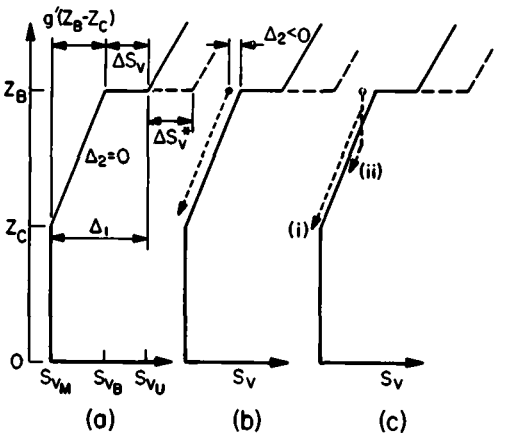

Fig. 3. Virtual static energy profiles, illustrating (a) relationships among cloud stratification, inversion strength and Δ_1 (this is constructed such that $\Delta_2 = 0$); (b) s_v profile (dashed) of a new *saturated* mixed layer forming under the inversion when $\Delta_2 < 0$; (c) s_v profiles of new *unsaturated* mixed layers when saturation occurs (i) above and (ii) below neutral buoyancy. Case (cii) is potentially stable.

Fig. 3a shows the relationships derived in Section 2a. Here, $\Delta_2 = \Delta s_v - \Delta s_v^* = 0$. Fig. 3b illustrates the mixing of saturated parcels to form a new mixed layer on the cloud; since the mixing produces values of $s_v < s_v(z)$ it then proceeds unimpeded. This corresponds to Deardorff's (1980) experiment. Fig. 3c shows two possible results of mixing in unsaturated parcels. If they saturate above their neutral buoyancy level they can proceed unimpeded (case (i)), but if they cross the existing stratification before saturation (case (ii)), further mixing produces potential energy and they may not be enough TKE available to erode entirely through the pre-existing cloud. It should be remarked here that the zero-buoyancy levels in Figs. 3b and 3c are not related to the discussion of Subsection 3.1. That case referred to a layer well-mixed from the surface to the inversion; this case pertains to a secondary mixed layer forming below the inversion.

4. Conclusion

This paper is concerned with distinguishing between cloud-top TKE generation associated with

entrainment fluxes (Deardorff's (1980) "cloud-top entrainment instability" and Randall's (1980) "conditional instability of the first kind upside-down") and processes or conditions that are sufficient to lead to the break-up of a solid stratocumulus deck, which is called here "stratocumulus instability." The motivation for making this distinction is two-fold. First, diagnosing and forecasting stratocumulus instability correctly are necessary both for climate and weather modelling and for operational use. Second, the data and model analyses presented here show that cloud-top entrainment instability may not necessarily lead to stratocumulus instability.

Problems associated with diagnosing stratocumulus instability as measured by inversion jumps of thermodynamical variables were discussed in Section 2, and the conclusion of Mahrt and Paumier (1982), that small-scale variability and uncertainty in measurements makes such diagnoses imprecise, was corroborated with a larger data set. Large negative values of the stability parameter Δ_2 (see eq. 2.5) do indeed correlate with broken stratocumulus, as do large positive values with solid stratocumulus, but, from the data in Section 2, it could not be determined at what point the switch-over occurs: anomalous cases represented ~43% of the total.

The most obvious physical mechanism for stratocumulus instability is the generation of TKE by the entrainment fluxes in such a manner as to cause ever increasing entrainment rates ("runaway entrainment"). A simplified mixed-layer model, with the entrainment closure developed by Stage and Businger (1981a, b), was used to investigate this process. The simplest possibility for runaway entrainment is that the overall layer stability (Ψ) vanishes; in this entrainment closure, this coincides with the onset of cloud-top entrainment instability ($\Delta_2 \leqslant 0$) only when the cloud base occurs at the surface. Elevated cloud bases require substantially negative values of Δ_2 for Ψ to vanish, in agreement with the closure of Deardorff (1976). Befor Ψ vanishes, the inversion may become statically unstable ($\Delta s_v < 0$ in eq. 2.8), however, and examination of the behavior of Ψ as deduced from the thermodynamic budget equations shows that this is indeed a candidate for stratocumulus instability. It does not, however, explain the results of Deardorff's (1980) numerical experiment or the unstable cases in the 1981 data. Otherwise, the behavior of Ψ (for fixed cloud geometry) is intrinsically stable.

The most appealing explanation of stratocumulus instability based on the results presented here was first suggested by Deardorff (1980), and concerns competition between drying out of the cloud due to entrainment of drier air from above and moistening due to mixing of wetter air from below. The mixed-layer model was used analytically to investigate the ratio of the time scales for these processes and its was found that the drying becomes increasingly dominant for values of $\Delta_2 < 0$ ($\psi < 1$ in Fig. 2). However, for slightly negative Δ_2, the behavior is not much different from slightly positive values. This behavior is consistent with Deardorff's (1980) calculations and with the data in Section 2. It is also consistent with the internal circulation processes of an Sc-topped mixed layer. It appears that this comparison of time scales could be used to diagnose stratocumulus instability and that it may have forecasting potential.

An important aspect of the numerical experiment by Deardorff (1980), that the vertical fluxes are no longer linear with height after the onset of cloud-top entrainment instability and hence mixed layer models are no longer valid, raises several questions that require further numerical modeling to answer. The heuristic explanation of the flux profiles given here provides a physical basis for the design of future experiments. The onset of cloud-top entrainment instability raises the TKE level in the upper part of the cloud layer and results in a sort of secondary mixed layer atop the pre-existing one. Whether or not this new layer penetrates through the cloud (causing stratocumulus instability) or not depends on the cause of the cloud-top entrainment instability. In Deardorff's (1980) experiment, it was caused by *cooling* of the above inversion air; thus, the new "mixed layer" was saturated and could erode the old cloud (Fig. 3b). A useful experiment would force the cloud-top entrainment instability by *drying* the upper air. Would this then cause stratocumulus instability? It would also be useful to carry out an integration until a quasi-equilibrium has been re-established, i.e., until the new "mixed layer" reaches some steady state. Could stratocumulus instability be a temporary, intermediate adjustment stage between two stable Sc regimes?

The analysis in Section 3 with the fixed-geometry

mixed-layer model subject to fixed surface fluxes cannot be considered quantitative. Stage and Businger's (1981a, b) entrainment closure is attractive, due to its analytic tractability in the form used here, but other closure formulations are available and may produce different results. The inapplicability of a mixed-layer model to the post-cloud-top entrainment instability physics makes some of the analysis above even more suspect. Problems and expense of data acquisition make it questionable as to whether field experiments to investigate stratocumulus instability are justifiable at this stage. It would therefore seem that numerical experiments are mandated to further understanding of this important aspect of boundary layer mechanics.

5. Acknowledgment

This paper results from research supported by the National Science Foundation under Grant no. ATM 8209115 and by the National Oceanic and Atmospheric Administration through the Equatorial Pacific Ocean Climate Studies program, which also funded the research flights discussed here. I thank Naomi Ware for processing the manuscript.

6. Appendix A

Symbols

Symbol	Meaning	Introductory eq. no.
A	fraction of turbulence not dissipated	(3.20)
A'	A associated with positive cloud-top buoyancy flux	(3.21)
B	as subscript, value just below inversion base (at cloud top)	(2.5)
B_0	Bowen ratio	(3.19)
C	constants or unspecified functions; as subscript, lifting condensation level (cloud base) value	(2.9)
c_p	specific heat of air at constant pressure	(2.2)
$F_{h,q}$	surface flux of h, q	(3.16)
F_R	cloud-top radiative flux	(3.16)
F	entrainment forcing function	(3.17)
$F_{1,2}(F_{1,2,\phi})$	linear combinations of F's (F's)	(3.18) (B.2, B.4)
$f_{U,M}$	mixing fractions; $f_U + f_M = 1$	(3.1)
g	gravitational acceleration	(2.2)
g'	$\partial s_v/\partial z$ in cloud layer	(2.4)
$H_{h,r}$	upper air advective terms for h, r	(B.1)
$H_{1,2}$	linear combinations of $H_{n,r}$	(B.2)
h	moist static energy	(2.2)
I	as subscript, intermediate parcel value	(3.1)
L	latent heat of condensation	(2.2)
l	liquid water mixing ratio	(2.1)
M	as subscript, mixed layer value	(3.1)
q	water vapour mixing ratio	(2.1)
r	total water mixing ratio ($q + l$)	(2.1)
s_v	virtual static energy (analog of virtual potential temperature)	(2.4)
T	temperature	(2.2)
T	ratio of cloud-top moistening/drying time scales	(3.31)
t	time	(3.16)
w_e	cloud-top entrainment velocity	(3.16)
w_*	mixed-layer convective velocity scale	(3.30)
z	height	(2.2)

$\hat{z}$	non-dimensional height in cloud layer	(3.5)
α	ratio of $L\Delta r/\Delta h$ for runaway entrainment	(3.23)
β	thermodynamic coefficient (ratio of moist/dry lapse rates)	(2.3)
$\Gamma_{1,2,\Phi}$	linear combination of $\gamma_{h,r}$	(B.2, B.4)
γ	thermodynamic coefficient (proportional to $\partial q^*/\partial T$)	(2.3)
$\gamma_{h,r}$	above-inversion $\partial(h, r)/\partial z$	(A.2.1)
$\Delta(\ )$	inversion jump ($\Delta h \equiv h_U - h_B$, etc.)	(2.6)
$\Delta_{1,2}$	Linear combinations of Δh, Δr	(2.5), (2.8)
Δs_v^*	"critical value" of Δs_v below which $\Delta_2 < 0$	(2.7)
δ	virtual temperature correction factor	(2.3)
ε	thermodynamic coefficient	(2.3)
ϑ_v	virtual potential temperature	before (2.4)
ϑ_R	reference potential temperature	(3.30)
ζ	z_C/z_B	(3.18)
$\tau_{m,d}$	moistening, drying time scales	(3.31)
Ψ	overall layer stability	(3.17)
Ψ_0	steady-state Ψ	(3.27)
ψ	zero-buoyancy level for $(\ )_1$ parcel	(3.7)
$(\ )^*$	saturation value	(2.1)
$(\cdot)$	Lagrangian time derivative	(3.16)
$(\ )_{1,2,\Phi}$	linear combinations; e.g.,	
	$F_1 = F_h - (1 - \varepsilon\delta)LF_q$	(B.2)
	$F_2 = \beta F_h - \varepsilon L F_q$	(B.2)
	$\mathbf{F}_\Phi = \zeta^2\mathbf{F}_1 + A'(1 - \zeta^2)\mathbf{F}_2$	(B.4)

7. Appendix B

Derivation of eq. (3.25)

The first-order, non-linear differential equation for Ψ, eq. (3.25), involves various definitions and two main assumptions. Since an explicit solution is not attempted, the full system of equations for Ψ, z_B, and z_C is not considered.

The above-inversion moist static energy and water vapor are assumed to vary according to

$$\dot{h}_U = w_e\gamma_h + H_h, \qquad \text{(B.1)}$$

$$\dot{r}_U = w_e\gamma_r + H_r,$$

where the above inversion gradients are given by $\gamma_{h,r}$ and where the second terms are horizontal advections such as that imposed in Deardorff's (1980) numerical experiment.

Defining

$$\Gamma_1 \equiv (\gamma_h - (1 - \varepsilon\delta)L\gamma_r)z_B,$$

$$\Gamma_2 \equiv (\beta\gamma_h - \varepsilon L\gamma_r)z_B,$$

$$H_1 \equiv H_h - (1 - \varepsilon\delta)LH_r,$$

$$H_2 \equiv \beta H_h - \varepsilon L H_r, \qquad \text{(B.2)}$$

$$\mathbf{F}_1 = F_1 - F_R - z_B H_1$$

$$\mathbf{F}_2 = F_2 - \beta F_R - z_B H_2,$$

the mixed layer budgets and the entrainment closure may be combined with eqs. (B.1) to give

$$\dot{\Delta}_1 = \frac{\mathbf{F}}{\Psi z_B}(\Gamma_1 - \Delta_1) - \mathbf{F}_1/z_B,$$

and

$$\dot{\Delta}_2 = \frac{\mathbf{F}}{\Psi z_B}(\Gamma_2 - \Delta_2) - \mathbf{F}_2/z_B. \qquad \text{(B.3)}$$

With the obvious additional definitions

$$\Gamma_\Phi \equiv \zeta^2\Gamma_1 + A'(1 - \zeta^2)\Gamma_2,$$

$$\mathbf{F}_\Phi \equiv \zeta^2\mathbf{F}_1 + A'(1 - \zeta^2)\mathbf{F}_2, \qquad \text{(B.4)}$$

these combine to give eq. (3.25) of the text:

$$\dot{\Psi} = \frac{\mathbf{F}}{z_B\Psi}(\Gamma_\Phi - \Psi) - \mathbf{F}_\Phi/z_B. \qquad \text{(B.5)}$$

It should be noted that, while eqs. (B.3) form a

closed set (given z_B and z_C), eq. (B.5) does not because A' depends on Δ_2 alone. The explicit steady-state values in the main text are chosen from the set of 2 values of (Ψ_0, Δ_{1_0}, Δ_{2_0}) calculated using $A' = (A, 1.0)$ based on consistency with eq. (3.22) in the text. In any case, choosing $A' = 1.0$ and using only eq. (B.5) in a search for instabilities implies physically, that the TKE generated by cloud-top entrainment instability is all used for potential energy generation elsewhere (none is dissipated).

In eq. (B.5), the forcing $\mathbf{F}$ is positive definite; this is the TKE generation by surface fluxes and radiation. On the other hand, it can be seen from the definitions (B.3) and (B.4) that $\mathbf{F}_\phi$ can be positive or negative according to the relative strengths of the imposed fluxes and advections. For realistic upper-air profiles, the stability, $\Gamma_\phi > 0$.

REFERENCES

Betts, A. K. 1983. Thermodynamics of mixed stratocumulus layers: saturation point budgets. *J. Atmos. Sci. 40*, 2655–2670.

Deardorff, J. W. 1976. On the entrainment rate of a stratocumulus-topped mixed layer. *Q J. R Meteo. Soc. 102*, 563–582.

Deardorff, J. W. 1980. Cloud top entrainment instability. *J. Atmos. Sci. 37*, 131–147.

Hanson, H. P. 1981. Note on stratocumulus instability. *Tellus 33*, 109–112.

Hanson, H. P. 1982a. Note on mixed-layer entrainment closure. *J. Atmos. Sci. 39*, 470–473.

Hanson, H. P. 1982b. EPOCS 1981 Summary Data Report. NOAA TM ERL-ESQ. 1. 157 pp. (Available from the author.)

Hanson, H. P. 1984. On mixed-layer modeling of the stratocumulus-topped marine boundary layer. *J. Atmos. Sci. 41*, in press.

Hanson, H. P. and Gruber, P. L. 1982. Effect of marine stratocumulus clouds on the ocean-surface heat budget. *J. Atmos. Sci. 39*, 897–908.

Kraus, E. B. and Leslie, L. D. 1982. The interactive evolution of the oceanic and atmospheric boundary layers in the source regions of the trades. *J. Atmos. Sci. 39*, 2760–2772.

Lilly, D. K. 1968. Models of cloud-topped mixed layers under a strong inversion. *Q J. R Meteo. Soc. 94*, 292–309.

Mahrt, L. and Paumier, J. 1982. Cloud-top entrainment instability observed during AMTEX. *J. Atmos. Sci. 39*, 622–634.

Moeng, C.-H. 1979. Stability of a turbulent cloud layer within the planetary boundary layer. Ph.D. dissertation, University of California at Los Angeles, 143 pp.

Moeng, C.-H. and Arakawa, A. 1980. A numerical study of a marine subtropical stratus cloud layer and its stability. *J. Atmos. Sci. 37*, 2661–2676.

Randall, D. A. 1976. The interaction of the planetary boundary layer with large-scale circulations. Ph.D. dissertation, University of California at Los Angeles, 247 pp.

Randall, D. A. 1980. Conditional stability of the first kind upside-down. *J. Atmos. Sci. 37*, 125–130.

Schubert, W. H., Wakefield, J. S., Steiner, E. J. and Cox, S. K. 1979. Marine stratocumulus convection. (I) Governing equations and horizontally homogenous solutions. *J. Atmos. Sci 36*, 1286–1307.

Stage, S. A. and Businger, J. A. 1981a. A model for entrainment into a cloud-topped marine boundary layer. (I). Model description and application to a cold-air outbreak episode. *J. Atmos. Sci. 38*, 2213–2229.

Stage, S. A. and Businger, J. A. 1981b. A model for entrainment into a cloud-topped marine boundary layer. (II). Discussion of model behavior and comparison with other models. *J. Atmos. Sci. 38*, 2230–2242.